ExHFT-7
28 June – 03 July 2009, Krakow, Poland

HEAT TRANSFER ENHANCEMENT IN DUCTS DUE TO ACOUSTIC EXCITATION

G. Bennett*, J. Mahon, D. Murray, T. Persoons, I. Davis
University of Dublin, Trinity College, Dublin 2, Ireland

ABSTRACT. The thermoacoustic effect that results from the interaction of a sound wave in a compressible fluid in contact with solid boundaries is known to be capable of removing heat from power dissipating systems. In this paper the standing wave acoustic field that is generated in an open ended duct, a section of which is heated, and how it interacts with the aerodynamic flow field is examined by an experimental study. Specifically, the effect the fluctuating acoustic pressure and associated particle velocity have on the internal fluid dynamics is investigated. The ultimate goal is to fully understand and optimize the interaction mechanisms in order to enhance the overall convective heat transfer from a heated duct to internal flow. An experimental rig which has been designed and built allows the fundamental fluid dynamic, acoustic and heat transfer mechanisms to be studied. The rig consists of a circular duct with a central copper isothermally heated section which is instrumented with thermocouples, a heat flux sensor, microphones and a cross-wire probe. The cross wire is used to measure both time varying temperature and velocity at a high frequency and spatial resolution and a calibration procedure which allows the sensor to measure fluctuating velocity at elevated temperatures is reported. Results from the current investigation demonstrate how convective heat transfer from the heated duct section to the internal flow is enhanced due to acoustic excitation. In this preliminary, investigative study, it is suggested that two different heat transfer mechanisms are identified: one associated with the increased turbulent mixing due to the added particle velocity; the second associated with acoustic streaming. The results show significant increases in flow temperature and heat transfer coefficients for free and forced convection regimes.

Keywords: Convective Heat Transfer, Duct Acoustics, Standing Wave

INTRODUCTION

Thermal management remains today one of the most important bottlenecks in the further development of electronic devices. Whilst new approaches, such as heat pipes and thermoelectric cooling technologies, are being developed, forced convection is still a necessary technique. As acoustic power is approximately proportional to (flow velocity)^6 to (flow velocity)^8 it is crucial that fan performance be optimised. The acoustic penalty for an increase in flow velocity is addressed in this paper, as an effective means to reduce the noise created by the fan would facilitate increased heat transfer. The long term goal of this exploratory work aims to address the following question ***"To what extent can the existing noise from fans in electronics' thermal management systems be optimized to enhance convective cooling?"***

The 2006 market report by the European Electronic Component Manufacturers Association (EECA) shows [1, 2] that the European market for electronic components is worth in excess of €45 billion. The global semiconductor market grew by over 11.5% in the first half of 2006, covering the areas of power transmission, telecommunications, computers and peripherals, automotive and

* Corresponding author: Dr. Gareth Bennett
Phone: + (353)-1-8961383, Fax: + (353)-1-6795554
E-mail address: gareth.bennett@tcd.ie

aerospace [3]. The industry supports over 207,000 direct jobs in the EU [1], and many more indirect jobs.

Current fan-based forced convection techniques[4] with high performance heat sinks are capable of cooling up to 13 W/cm^2. For microprocessors, the heat dissipation is still increasing exponentially, while current processor designs are around the limit of 15 W/cm^2 corresponding to the forced air cooling bottleneck[5]. Since the current integrated circuits are pushing the power boundary, new cooling technologies are being examined. In telecommunications, the maximum power density is currently around 24 W/cm^2, requiring heat pipes to spread the heat to a larger surface area[6]. Present thermoelectric cooling technology[7] is limited to a power density of about 10 W/cm^2, although more advanced materials are being developed to increase the power density to beyond 500 W/cm^2. However, this is an expensive solution with a limited relevance for broad range applications.

The substantial research effort going into removing the heat generated by the electronic circuitry, using advanced methods such as heat pipes or liquid cooling provides an effective way of transporting the heat away from the confined chip geometry to a larger heat-sink with fan, where the heat is more easily transferred to the surrounding air. Crucially, the use of advanced high heat flux cooling methods does not eliminate the need for fan-based air cooling. This is the framework for the proposed research, which aims to use fan noise in a constructive way, to enhance convective heat transfer in thermal systems.

The thermoacoustic streaming theory initiated by Lord Rayleigh[8] has excited researchers and engineers for over one hundred years. The thermoacoustic instability observation of Rijke's Tube that Rayleigh's theory was able to explain, is found today in pulse combustor engines and low NOx aero-engine multi-stage annular combustors, and attempts to computationally model the phenomenon continue[9, 10]. Since Rayleigh, more recent fundamental theoretical studies have been carried out by Karimi et al.[11], and Swift[12, 13] and Garrett[14] in the area of thermoacoustics applied to refrigeration. The theoretical acoustic enhancement of heat transfer to particles and droplets such as pulverized coal particles and coal-water slurry fuel droplets[15, 16] has been examined as have experimental studies for configurations such as enclosures[17], parallel plates[18], flow over cylinders[19], heated wires[20] and impinging jet flows[21, 22]. Recently, the phenomenon has been applied to cooling of products within the electronics industry by Komarov and Hirasawa[20], and Lee and Loh[23] and to plasma screens by Kim at al.[24].

A fundamental experimental study on the heat transfer enhancement in ducts due to the acoustic excitation of axial fans is proposed in this project. The results of the work will find application in thermoacoustic refrigeration, heat transfer in ducts and in the electronics sector.

EXPERIMENTAL SETUP

General rig layout

The principal element of the experimental rig is a vertically oriented circular duct of an overall length equal to 2.944m and an internal diameter of approximately 0.1m. The duct, as shown in figure 1, consists of three parts: lower and upper sections of PMMA (Polymethyl Methacrylate) and a central section of copper. The transparent PMMA was chosen for its low thermal conductivity and for its suitability for future PIV measurements. The wall thickness is 10mm with an internal diameter of 100mm. The central copper section of 0.520m length and 1.5mm wall thickness was chosen for its high thermal conductivity and is mounted to a support frame via an Ertalon 6 PLA flange of 10mm thickness clamped at each end. The copper section thus butts against the PMMA at both ends and is in contact with just the two low conductivity 10mm thick Ertalon flanges. This mounting arrangement was designed to reduce conductive heat loss from the copper section which is heated on its external surface by a Holroyd 1.5 kW H/SR-PA silicon heater mat over the length between the flanges of 0.5m. The mat is powered by a RegaVolt Variac, and the current to the mat is monitored via a multi-meter which allows the power input to be measured. The schematic also shows the copper pipe to be instrumented with two T-type thermocouples, which are mounted, at either end, flush with the inside of the pipe surface. Three 6mm holes were cut through the heater mat and copper piping along its length to allow for access of the cross-wire anemometer and for microphone pressure measurements, with any unused holes blocked during testing. A type 27036 RdF Micro-foil heat-flux sensor with integral T-type thermocouple is placed mid-point of the total length of the pipe which is 9.1mm below the top cross-wire hole. As a right-angled cross wire was employed to ensure no disturbance to the flow field by the hot wire support, the 9.1mm length corresponds to the extension of the cross-wire normal to the probe. This set up allows for temperature and velocity profiles to be measured at the same mid-point axial location as the heat flux sensor.

A D.C. tube-axial fan is mounted at the top of the duct and is used to control the fluid velocity through the pipe. In addition to the cross-wire velocity measurements, a pitot-static tube was used to monitor average flow velocities. A 600W JBL 2206 H speaker is located at the lower end of the duct and is used to introduce pressure fluctuations at set frequencies. A gap between the speaker and the duct allows air to be drawn up through the duct for forced convection tests.

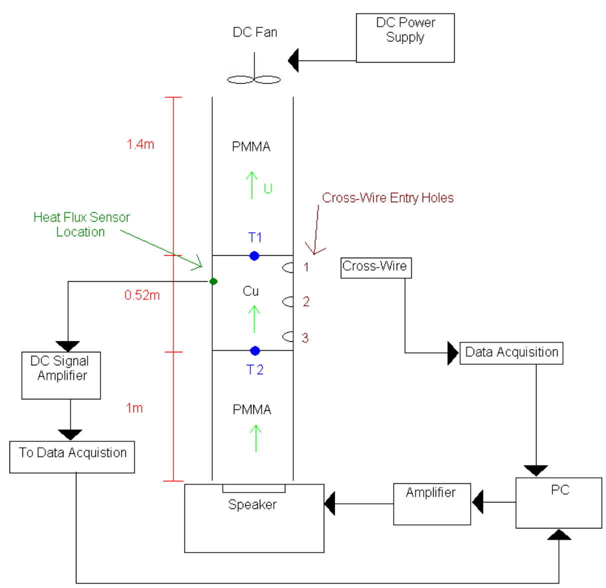

Figure 1. Experimental test rig

Instrumentation

A Dantec X-probe type 55P63, with a right angle between the sensor and the probe holder, is used to obtain velocity and temperature measurements. One of the wires of the cross-probe is used to measure fluctuating velocity obtained using a Dantec StreamLine Constant Temperature Anemometer (CTA). The other 'cold-wire' is configured to act as a resistance thermometer using constant-current anemometry (CCA) the temperature of which is determined by an accurate measure of its resistance.
The radial position of the cross-wire is accurately controlled by a linear actuator attached to a stepper motor which was calibrated to ensure spatial precision. The micro-foil sensor signal, of the order of μV, is amplified x1000 using an Omega Omni-Amp III DC Signal Amplifier. The thermocouples are connected to an Omega Toggler device which displays the temperature on-screen. The DC fan used is powered by a Thurlby 30V-1A DC power source. The speaker used to introduce the standing wave receives a signal from a QSC Power amplifier, which in turn receives a signal from .wav files

generated in Matlab and output via LabView through a National Instruments D/A converter. All data from the heat-flux sensor, the cross-wire and the microphones are acquired by a National Instruments data acquisition system, using N.I.'s LabView and and Dantec's StreamWare software on a Dell Precision T3400 PC. A LabView programme was written to automate control of the speaker frequency, the cross-wire location via the stepper motor and data acquisition of the heat flux sensor and cross-wire measurements.

Cross-Wire Calibration

Hotwire anemometry is based on convective heat transfer from a heated wire. However, in this test setup the temperature of the fluid may vary with time and/or is at a different temperature to nominal ambient temperature at which the hotwire was calibrated. As the principle underlying the measurement of flow velocity is based on heat transfer it is necessary to measure the actual temperature of the flow and hence correct for the temperature difference.

There are a number of approaches to correct the velocity for elevated temperature. The simplest method is based on the assumption that heat transfer from the probe is proportional to the temperature difference (between the wire and ambient temperature) and the relationship is shown in equation 1

$$E_{corr} = \left(\frac{T_w - T_0}{T_w - T_a} \right)^{\frac{1 \pm m}{2}} E_a \qquad (1)$$

where E_a = acquired voltage, E_{corr}= temperature corrected voltage, T_w=hotwire measurement, T_0= ambient reference temperature, T_a= fluid temperature during calibration and m = temperature loading factor, which is a dimensionless physical material property (for air, m = 0.16).

A more accurate approach for calibrating the hotwire is direct calibration of the hotwire at the ambient temperature of the fluid under test. In the current study both the fluid velocity and temperature vary significantly, hence direct calibration was the most accurate and appropriate method. A discussion of this approach can be found in Bearman[2].

The accuracy of the results from the hotwire anemometry system is dependent on both the acquired voltage (velocity) and temperature of the fluid. Hence, it is important to measure both simultaneously. Both quantities were measured using a cross wire probe, type 55P63. The method of temperature measurement used in this paper is based on a resistance thermometer. The temperature measurements were obtained from the resistance measurement of wire 1. Wire 2 was used to measure flow velocity using a standard constant temperature anemometer.

The resistance wire was calibrated by exposing the wire with flow at a known temperature and fitting a curve between temperature and measured resistance. A linear relationship was measured between the two quantities. Equation 2 shows the relationship between wire resistance and temperature. This was the basis for the temperature measurement.

$$R = R_0 \left[1 + \alpha (T - T_0) \right] \qquad (2)$$

where R is the wire resistance at temperature T, R_0 is the wire resistance at the reference temperature T_0 and α is the temperature coefficient of resistance.

The velocity and temperature sensitivity of the hotwire were obtained by operating the hotwire at a fixed overheat ratio of 1 and hence a fixed wire resistance. The hotwire system was balanced at an ambient temperature of *20.1°C*. The output voltage was recorded as a function of velocity and fluid temperature by using a specially designed calibration rig as shown in figure 2. The calibration was performed at a range of flow velocities ranging from 1m/s to 7m/s at four ambient temperatures of 20, 30.1, 39.8 and 50.1°*C*. The set of calibration data are shown in figure 3. A fourth order polynomial was used to fit the data as per equation 3.

$$U = C_0 + C_2 E + C_2 E^2 + C_3 E^3 + C_4 E^4 \tag{3}$$

where C_0 to C_4 are the calibration constants and E is the anemometer voltage.

The cross-wire as a sensor was chosen as an attractive solution for temperature and velocity measurement as high spatial and frequency resolutions could be achieved at almost coincident positions. In addition, as both wires were contained within the one holder, a good aerodynamic seal could be obtained at the sensor/copper duct interface. However, due to these proximate locations, tests had to be conducted to ensure that the "cold-wire" was not influenced by the presence of the hot wire, i.e. the "cold-wire" measured the fluid temperature independently of the hot-wire temperature. Tests were conducted to determine the influence of operating the hot-wire (*286°C*) on the resistance wire for a range of ambient temperatures (*20*, *40* and *60°C)* and for two flow velocities of 2m/s and 3m/s. The values chosen are comparable to the parameters under test. It was found that the temperature fluctuated about a mean value and that the variation in measurement with and without the hot-wire operating was consistent with random experimental error.

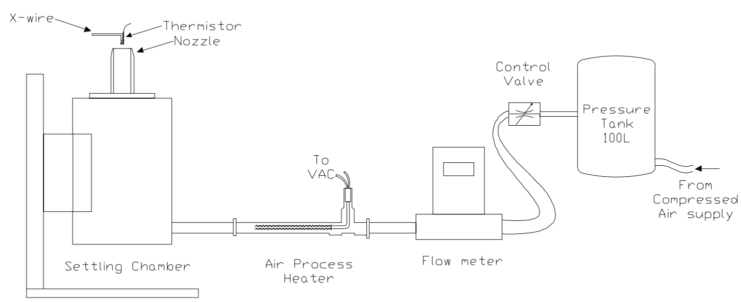

Figure 2. Rig to calibrate "cold-wire" for temperature measurement and the hot-wire for temperature corrected velocity measurement.

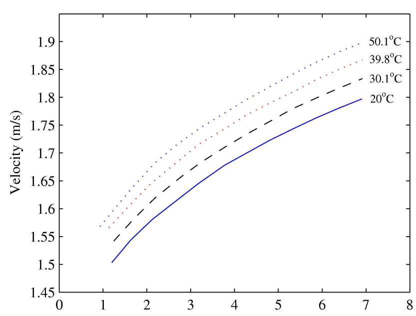

Figure 3. The dependence of hot-wire voltage on flow velocity at a number of ambient temperatures

Hydrodynamic, Thermal and Acoustic Considerations

For the forced convection tests discussed in this paper the mean velocity was measured to be 1.93m/s which for air in a duct of diameter 0.1m results in a Reynolds number of 12,841. Being greater than 10,000, the flow is considered to be fully turbulent. The axial measurement position of the heatflux sensor and cross-wire was located at the downstream end of the heated section. This results in x/D≈15 from the entrance of the duct and x/D≈5 from the beginning of the heated section.

The upper section of the duct was thus increased in length so that the heatflux sensor was located at exactly the midpoint of the total duct length. Fixing the measurement plane at the centre of the pipe allowed acoustic pressure or particle velocity nodes and anti-nodes to be easily aligned at this plane. By exciting the duct with random noise, and measuring its response with a microphone located flush with the inside of the duct wall, the duct resonant modes could be measured. These frequencies agreed closely with the theoretical resonant modes for an open ended duct according to the equation

$$f_n = n\left(\frac{c}{2(L+\Delta)}\right) \tag{4}$$

where Δ is an end correction to account for the radiation impedance at the end of an open duct. Δ =(D/2)*z, where z is a function of the flange size at the termination. For our rig z is approximately equal to 0.61. Figure 4 shows an illustration of the first four resonant frequencies examined in our duct and how the normalised pressure distribution, in blue and normalised particle velocity distribution, in red, vary along its length. The heat flux sensor is indicated by a small black square towards the end of the heated section at the midway point. Frequencies 63Hz and 167Hz result in particle velocity nodes at the measurement plane, whereas 113Hz and 223Hz result in particle velocity antinodes.

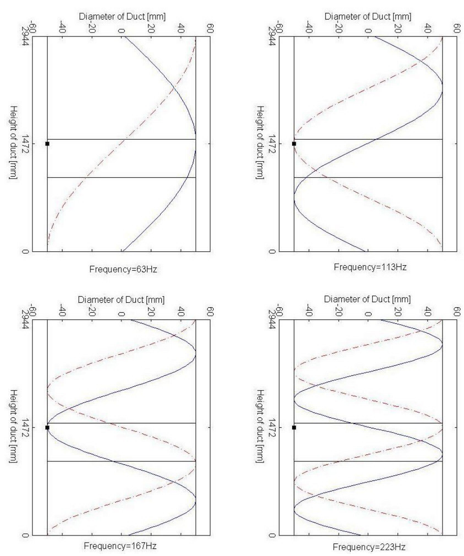

Figure 4. Acoustic pressure (blue) and particle velocity (red) distributions along the length of the duct for the first four resonant modes of the duct.

RESULTS AND DISCUSSION

Temperature, velocity and heat flux measurements were taken at the mid point of the duct (the measurement plane) for a series of experimental configurations. The main variables were: wall temperature [ambient, hot]; flow [free convection, forced convection]; frequency [0Hz, 63Hz, 113Hz, 167Hz, 223Hz]. For free convection the wall temperature was 78.8°*C* whereas for forced convection the temperature was 60.4°*C*. As both 63Hz and 167Hz result in particle velocity nodes at the measurement plane, these shall be referred to as N1 and N2 where as frequencies 113Hz and 223Hz will be referred to as A1 and A2, due to the fact that particle velocity is a maximum at this location. Figure 4 shows the effect that the standing wave has on the time averaged temperature profile for both free and forced convection configurations. For the free convection situation, the added sound serves to reduce the temperature near the duct wall (8-4mm from the wall) whereas the temperature in the main body of the flow increases significantly. A2 differs in a band centred at 10mm from the wall where the temperature is particularly elevated - an increase of 50-80%. For the forced convection case, an increase in mean temperature is again to be seen but this time the effect is localised to bands near the wall, the centre distance of which changes with frequency. Again, the temperatures decreases very close to the wall for all frequencies.

Figure 5 plots temperature corrected mean and fluctuating velocity readings for hot and cold wall temperatures for forced convection. These results show that N1 and N2 behave similarly to each other as do A1 and A2 and, at least qualitatively, for most positions there is little difference between the cold and hot wall conditions. From observation of the fluctuating velocity of frequencies A1 and A2, the particle velocity can be quantified as approximately 0.4m/s at the measurement plane. As the plane wave cut-off frequency for this diameter duct is approximately 2kHz, all four frequencies considered generate plane wave standing waves and thus the particle velocity should increase uniformly across the diameter. This is clearly seen for frequencies A1 and A2, as expected with a slight difference close to the wall for the heated wall condition. In contrast for frequencies N1 and N2 the fluctuating velocity should be expected to remain unchanged as the location is at a velocity node. This is the case except, surprisingly, at banded distances from the wall where large increases in fluctuating velocity are measured. In the same bands for the same two N1 and N2 frequencies, the mean velocity is also seen to increase significantly. For all frequencies, the mean velocity also increases, to a varying extent, outside of these bands.

Qualitatively, the unusual banded behaviour is suggested to be caused by acoustic streaming where two different types of circulatory flow structures may be generated: “Rayleigh” structures generated outside viscous boundary layers and a second streaming “Schlichting” structure generated in the immediate vicinity of the viscous boundaries. In the results presented in this paper, the Rayleigh structure is thought to be identifiable for the N1 and N2 frequencies. Some qualitative differences between the hot and cold wall conditions close to the wall might be attributed to Schlichting structures but further testing needs to be done to verify this. If this is the case, these circulatory structures serve to remove heat from the wall surface and to circulate this heat into the flow where it is exhausted with the mean flow. Whereas acoustic streaming is normally restricted in the literature to closed ended ducts, the experimental setup described here benefits from the fact that standing waves can be generated in open ended ducts at low frequencies.

Figure 6 summarises these results for the hot wall case from the point of view of heat transfer. For the no flow case the mean temperature is plotted as a function of frequency whereas for the forced convection case both the mean temperature and a mass-flow rate averaged temperature (bulk temperature) is presented. The bulk temperature is calculated according to equation (5)

$$T_b = \frac{\sum_{j=1}^{N}\left(T_j \times U_j\right)}{\sum_{j=1}^{N} U_j} \tag{5}$$

where j is a measurement location. For the free convection case, the average temperature increases due to acoustic excitation, markedly at A1, whereas for forced convection only N1 and N2 result in a temperature increase.

Availing of the heat flux measurement, the convective heat transfer coefficient can be calculated according to equation 6.

$$h = \frac{q''}{(T_s - T_m)} \tag{6}$$

where Ts is a surface temperature and Tm is mean fluid temperature. In figure 6, results using both the mean temperature and the bulk temperature are used for comparison. However, unfortunately, due to an instrumentation error, the heat flux thermocouple failed. This means that an accurate measure of the surface temperature at the heat flux sensor as a function of frequency was not available. To overcome this, the “cold-wire” temperature closest to the heat flux sensor, which was approximately 1mm away was used. Using this approach, the heat transfer coefficients are presented relative to the 0Hz benchmark. Despite the erroneous surface temperature, qualitative similarities are apparent with the other data which give credence to the results. For the free convection case, remarkable increases in heat transfer coefficient are measured for all frequencies. For higher velocities again the N1 and N2 frequencies pair off as do the A1 and A2 frequencies, with the velocity node frequencies giving the greatest increase in heat transfer coefficient.

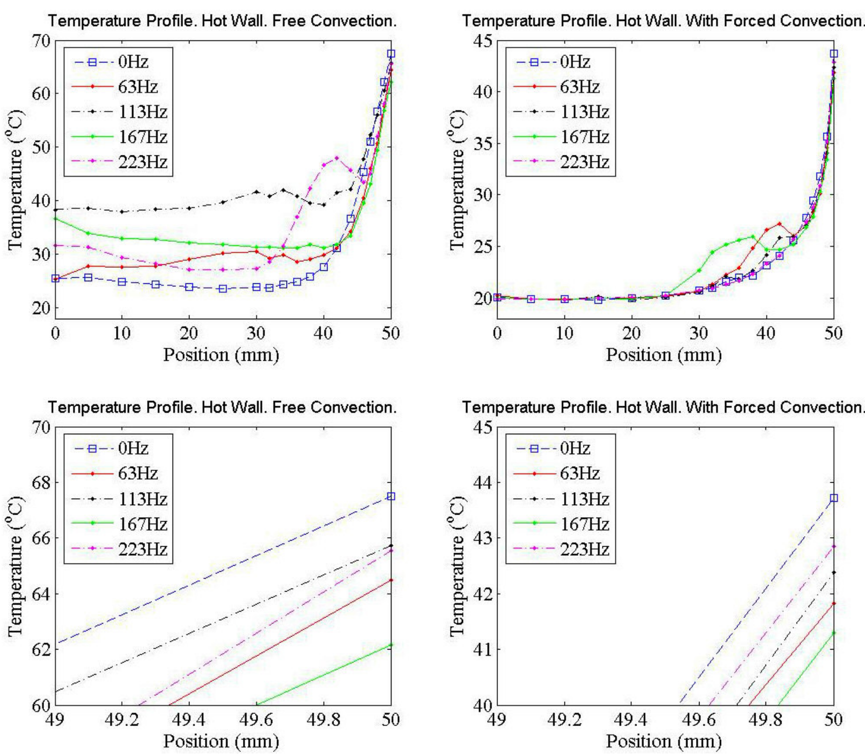

Figure 4. Time averaged temperature profiles over a radius of the duct at the measurement plane as a function of resonant mode frequency. The first figure is for a free convection condition with a wall temperature of *78.8°C*. The second plot is for forced convection with mean velocity of 1.94m/s and a wall temperature of *60.4°C*. The bottom two figures are close ups at the wall surface. The centre line of the duct corresponds to 0mm.

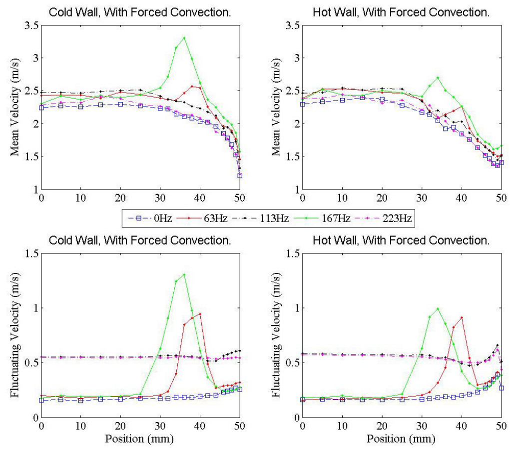

Figure 5. Mean and fluctuating velocity profiles as a function of frequency and wall temperature in the direction of flow.

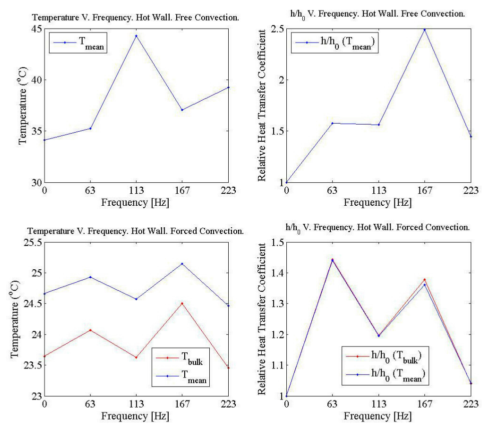

Figure 6. Averaged temperature and relative heat transfer coefficient as a function of standing wave frequency.

CONCLUSIONS

Temperature, mean velocity and fluctuating velocity distributions across the radius of a vertical heated open ended duct subject to acoustic excitation have been presented for forced and free convection cases. By exciting the duct at different standing wave resonant modes, the influence a particle velocity anti-node (pressure node) versus a particle velocity node (pressure anti-node) has on measurements at the same plane could be isolated. From the velocity results two principal heat transfer mechanisms are suggested. The first is due to an increase in particle velocity associated with the anti-node. This increase in fluctuation is aligned with an increase in turbulence and the resultant increase in turbulent mixing is seen to increase the heat transfer. The second mechanism is suggested, in this investigative work, to be attributed to acoustic streaming where two different types of circulatory flow structures may be generated. These sound induced heat transfer mechanisms coupled with free convection are seen to combine efficiently, serving to transport heat into the flow to be exhausted from the duct.

REFERENCES

1. *EECA Market Report 2006, European Electronic Component Manufacturers Association, 2006.*
2. Bearman, P.W., *Correction for the effect of ambient temperature drift on hotwire measurements in incompressible flow.* . DISA Information. 1971.

3. *World UPS Market Records Double-Digit Growth, 2006.*
4. Janssen, G., Kole, A., Leroux, A., *Trends in cooling of electronics: The use of thermal roadmaps*, in *Electronics Cooling*. Aug 2004.
5. M. J. Ellsworth, R.E.S., *High powered chip cooling: Air and beyond*, in *Electronics Cooling*. Aug 2005.
6. A. Vukovic, E.C., in *Communication network power efficiency: Assessment, limitations and directions*. Aug 2004.
7. K. Fukutani, Y.Z., A. Shakouri,, *Solid-state microrefrigerator on a chip*, in *Electronics Cooling*. Aug 2006.
8. Strutt, J.W.r.B.R., *The theory of sound*. 2nd ed. rev. and enl. ed. 1945, New York: Dover.
9. B. Entezam, W.K.V.M., J. Majdalanit, *MODELING OF A RIJKE-TUBE PULSE COMBUSTOR USING COMPUTATIONAL FLUID DYNAMICS*, in *33rd AIAA/ASME/SAE/ASEE Joint Propulsion Conference and Exhibit, AIAA-1997-2718* 1997: Seattle, WA.
10. hantschk c.-c., v.d., *Numerical simulation of self-excited thermoacoustic instabilities in a Rijke Tube.* Journal of Sound and Vibration, 1999. **227**(3): p. 511-522.
11. Karimi, N., M.J. Brear, and W.H. Moase, *Acoustic and disturbance energy analysis of a flow with heat communication.* Journal of Fluid Mechanics, 2008. **597**: p. 67-89.
12. Swift, G.W., *Thermoacoustic Engines.* Journal of the Acoustical Society of America, 1988. **84**(4): p. 1145-1180.
13. Swift, G.W., *Thermoacoustic Engines and Refrigerators.* Physics Today, 1995. **48**(7): p. 22-28.
14. Garrett, S.L., *Resource letter: TA-1: Thermoacoustic engines and refrigerators.* American Journal of Physics, 2004. **72**(1): p. 11-17.
15. Ha, M.Y. and S. Yavuzkurt, *A Theoretical Investigation of Acoustic Enhancement of Heat and Mass-Transfer .1. Pure Oscillating Flow.* International Journal of Heat and Mass Transfer, 1993. **36**(8): p. 2183-2192.
16. Ha, M.Y. and S. Yavuzkurt, *A Theoretical Investigation of Acoustic Enhancement of Heat and Mass-Transfer .2. Oscillating Flow with a Steady Velocity Component.* International Journal of Heat and Mass Transfer, 1993. **36**(8): p. 2193-2202.
17. Aktas, M.K., B. Farouk, and Y.Q. Lin, *Heat transfer enhancement by acoustic streaming in an enclosure.* Journal of Heat Transfer-Transactions of the Asme, 2005. **127**(12): p. 1313-1321.
18. Vainshtein, P., M. Fichman, and C. Gutfinger, *Acoustic Enhancement of Heat-Transfer between 2 Parallel Plates.* International Journal of Heat and Mass Transfer, 1995. **38**(10): p. 1893-1899.
19. Su, J.H., C. Gau, and C.S. Yang, *Enhancement of heat transfer over a cylinder by acoustic excitation.* Journal of Thermophysics and Heat Transfer, 2006. **20**(2): p. 256-266.
20. Komarov, S. and M. Hirasawa, *Enhancement of gas phase heat transfer by acoustic field application.* Ultrasonics, 2003. **41**(4): p. 289-293.
21. O'Donovan, T.S. and D.B. Murray. *Effect of acoustic excitation on the heat transfer to an impinging air jet (HT2007-32800).* in *ASME-JSME Thermal Engineering Summer Heat Transfer Conference*. 2007. Vancouver.
22. O'Donovan, T.S. and D.B. Murray. *Heat transfer to an acoustical excited impinging air jet*. in *Proceedings of the 5th European Thermal-Sciences Conference*. 2008. Eindhoven.
23. Lee, D.R. and B.G. Loh, *Smart cooling technology utilizing acoustic streaming.* Ieee Transactions on Components and Packaging Technologies, 2007. **30**(4): p. 691-699.
24. KIM, S.K., W.N. KIM, and S.Y. KIM, *Plasma display panel cooling by an acoustic pulsating flow device*, in *ITherm 2004 : (Ninth Intersociety Conference on Thermal and Thermomechanical Phenomena in Electronic Systems)* 2004, IEEE: Mirage Hotel & Casino, Las Vegas, NV, June 1-June 4, 2004